

Towards Understanding the Tandem Mass Spectra of Protonated Oligopeptides. 1: Mechanism of Amide Bond Cleavage

Béla Paizs and Sándor Suhai

Department of Molecular Biophysics, German Cancer Research Center, Heidelberg, Germany

The mechanism of the cleavage of protonated amide bonds of oligopeptides is discussed in detail exploring the major energetic, kinetic, and entropy factors that determine the accessibility of the b_x - y_z (Paizs, B.; Suhai, S. *Rapid Commun. Mass Spectrom.* **2002**, *16*, 375) and "diketopiperazine" (Cordero, M. M.; Houser, J. J.; Wesdemiotis, C. *Anal. Chem.* **1993**, *65*, 1594) pathways. General considerations indicate that under low-energy collision conditions the majority of the sequence ions of protonated oligopeptides are formed on the b_x - y_z pathways which are energetically, kinetically, and entropically accessible. This is due to the facts that (1) the corresponding reactive configurations (amide N protonated species) can easily be formed during ion excitation, (2) most of the protonated nitrogens are stabilized by nearby amide oxygens making the spatial arrangement of the two amide bonds (the protonated and its N-terminal neighbor) involved in oxazolone formation entropically favored. On the other hand, formation of y ions on the diketopiperazine pathways is either kinetically or energetically or entropically controlled. The energetic control is due to the significant ring strain of small cyclic peptides that are co-formed with y ions (truncated protonated peptides) similar in size to the original peptide. The entropy control precludes formation of y ions much smaller than the original peptide since the attacking N-terminal amino group can rarely get close to the protonated amide bond buried by amide oxygens. Modeling the b_x - y_z pathways of protonated pentaalanine leads for the first time to *semi-quantitative* understanding of the tandem mass spectra of a protonated oligopeptide. Both the amide nitrogen protonated structures (reactive configurations for the amide bond cleavage) and the corresponding b_x - y_z transition structures are energetically more favored if protonation occurs closer to the C-terminus, e.g., considering these points the Ala(4)-Ala(5) amide bond is more favored than Ala(3)-Ala(4), and Ala(3)-Ala(4) is more favored than Ala(2)-Ala(3). This fact explains the increasing ion abundances observed for the b_2/y_3 , b_3/y_2 , and b_4/y_1 ion pairs in the metastable ion and low-energy collision induced mass spectra (Yalcin, T.; Csizmadia, I. G.; Peterson, M. B.; Harrison, A. G. *J. Am. Soc. Mass Spectrom.* **1996**, *7*, 233) of protonated pentaalanine. A linear free-energy relationship is used to approximate the ratio of the b_x and y_z ions on the particular b_x - y_z pathways. Applying the necessary proton affinities such considerations satisfactorily explain for example dominance of the b_4 ion over y_1 and the similar b_3 and y_2 ion intensities observed for the metastable ion and low-energy collision induced mass spectra. (*J Am Soc Mass Spectrom* 2004, *15*, 103-113) © 2004 American Society for Mass Spectrometry

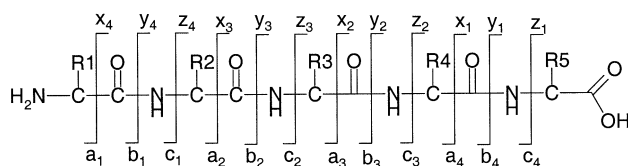
Mass spectrometry (MS) has recently become the method of choice for the analysis of biomolecules. This is mainly due to the development of soft ionization techniques such as electrospray ionization (ESI) [1] and matrix assisted laser desorption ionization (MALDI) [2] which introduce intact biomolecule ions into the gas-phase. MS is applied in the bio-sciences in mainly two ways: (1) for measuring the weight of proteins and peptides (peptide mass fingerprinting), and (2) for obtaining structural information

by fragmenting peptides generated by specific proteolytic enzymes using tandem MS (MS-MS) techniques. In the MS-MS experiments the ion (positive operation mode, e.g., protonated species) of interest is selected, excited to induce fragmentation, and the product ion spectrum is measured.

The information available in the MS-MS spectra of protonated peptides can be used to identify proteins in several ways. Amino acid residues can be determined from the mass difference of successive fragment ions of the same type (e.g., b_n and b_{n-1} , the nomenclature of references [3] and [4] is adopted in the present paper and is illustrated in Scheme 1), which corresponds to the mass of the residue by which they differ. In this way one can apply tandem mass spectrometry even for de

Published online November 19, 2003

Address reprint requests to Dr. B. Paizs, Department of Molecular Biophysics, German Cancer Research Center, Im Neuenheimer Feld 280, Heidelberg D-69120, Germany. E-mail: b.paizs@dkfz-heidelberg.de



Scheme 1

novo peptide sequencing provided the corresponding ion series are present in the MS-MS spectrum. Some algorithms make use of MS/MS data to generate "peptide-sequence tags" [5] that consist of information on the mass of the precursor and some of the fragment ions and of a short stretch of sequence. Another approach is based on in silico generation of MS-MS fragmentation patterns [6–8] for peptides derived from entries of protein and/or nucleic acid databases and comparison of the predicted spectra to those determined experimentally.

The intent to perform reliable large-scale proteomics studies is the major driving force of investigations of the fragmentation pathways of protonated peptides beside the basic academic interest. For example, derivation of "peptide-sequence tags" from the MS-MS spectra requires some knowledge of the major fragmentation pathways and rules. Since protonated peptides dissociate on a large number of different fragmentation pathways, making reliable predictions on the MS-MS spectra of peptides derived from entries of databases is an extremely difficult task. To make the situation even more complicated, some peptides show selective and/or enhanced fragmentation at some of the amino acid residues producing MS-MS spectra poor of valuable sequence ions. In the light of these facts it is not surprising that existing sequencing programs use only the information inherent the m/z values of the most important sequence ions and discard any intensity-related data. Protein identification using tandem mass spectrometry could no doubt be further refined if the major fragmentation laws of protonated peptides were known to such extent that they would permit predictions of some of the ion intensity relationships of the MS-MS spectra of protonated peptides.

The goal of the present paper and other papers in this series is to enhance our knowledge on the dissociation chemistry of protonated oligopeptides concentrating on the mechanism, energetics, and kinetics of cleavage of the amide bond. Our final aim with these studies is to derive the major rules determining the formation of sequence ions of protonated peptides. In the present paper we discuss the basic dissociation chemistry of protonated peptides by paying special attention to the charge-directed dissociation of the amide bond. For completeness, this discussion involves some mechanistic aspects already published on di- and tri-peptides but concentrates on those factors which influence and/or determine the major characteristics of amide bond cleavages in larger oligopeptides. The dissociation pathways of these peptides are discussed in general consid-

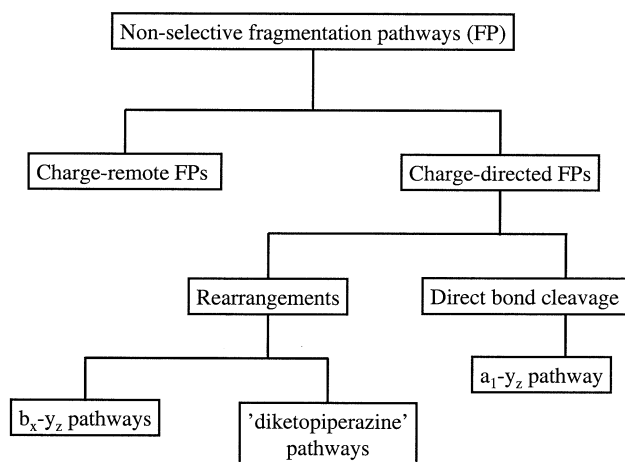
ering energetic, kinetic, and entropy factors. Finally, these considerations are worked out for the fragmentation pathways of protonated pentaalanine using high level quantum chemical and RRKM calculations. (Details of the applied computations are described in the Computational Details section of the paper.) This theoretical study permits *semi-quantitative* understanding of ion intensity relationships of the MS-MS spectra of protonated pentaalanine. According to our knowledge, this investigation represents the first successful attempt to explain the major factors determining the tandem mass spectrum of an oligopeptide.

Computational Details

To scan the potential energy surface (PES) of protonated pentaalanine we applied our recently developed conformational search engine devised specifically to deal with protonated peptides. These calculations started with molecular dynamics simulations on various protonated forms of AAAAA using the InsightII program (Biosym Technologies, San Diego, CA) in conjunction with the AMBER force field modified by us in order to manage amide nitrogen and oxygen protonated species. During the dynamics we regularly saved structures for further refinement by full geometry optimization using the same force fields. In the next step of the scan these structures were analyzed by our own conformer family search program. This program is able to group optimized structures into families for which the most important characteristic torsion angles of the molecule are similar. The most stable species in the families were than fully optimized at the HF/3-21G, B3LYP/6-31G(d) and finally at the B3LYP/6-31+G(d,p) levels.

Transition structures (TS) corresponding to various reactions were determined at the B3LYP/6-31G(d) and B3LYP/6-31+G(d,p) levels of theory. In most of the cases the transition structures obtained were checked by using intrinsic reaction path calculations (IRC) to unambiguously define which minima are connected by the TS investigated. Similar to the species belonging to the various protonation sites and transition structures, post-reaction complexes and proton-bound dimers were fully optimized at the B3LYP/6-31G(d) and B3LYP/6-31+G(d,p) levels of theory. Relative energies were calculated by using the B3LYP/6-31+G(d,p) total energies and zero-point energy corrections (ZPE) determined at the B3LYP/6-31G(d) level.

Using the results of these quantum chemical calculations (relative energies, vibrational frequencies, rotational constants), the unimolecular rate coefficients for some of the transitions were calculated using the RRKM method [9] over a grid of energies up to a limit well exceeding the calculated threshold energy of the lowest-energy fragmentation. It is known that the RRKM theory usually gives reasonable rate constants of various unimolecular reactions occurring during fragmentation of protonated peptides provided some minimal requirements



Scheme 2

in the quantum chemical calculations (theoretical level including correlation, average basis set) are fulfilled.

For all ab initio calculations the Gaussian [10] program was used.

Results and Discussion

We start our discussion by briefly reviewing the basic chemistry of amide bond dissociation which is then followed by presentation of mechanistic, energetic, and kinetic factors determining charge-directed formation of sequence ions of oligopeptides.

Dissociation of the Amide Bond—A Hierarchy of Pathways

The structurally most valuable fragment ions of protonated peptides are formed by cleavage of the amide bond and involve the b, y, and a ion series. (Scheme 1, sequence ions are members of the b, y, and a ion series, while ions derived by loss of small neutrals from protonated peptides are referred as non-sequence ions. Majority of a ions are formed by CO loss from b ions.) While b and y ions can be formed on both amino acid residue selective and non-selective fragmentation pathways, the present paper concentrates on the latter case.

The non-selective sequence ion pathways can be sorted into a hierarchy (Scheme 2) by analyzing the most important chemical aspects of the reactions involved. The formation of the b and y fragment ions can be described as a competition between charge-remote and charge-directed cleavages of the amide bonds in a very complicated reaction pattern where the amide bonds are cleaved with substantially different probabilities. Under low energy collision conditions the majority of the sequence ions are formed on charge-directed pathways which involve migration of the added (“mobile”) proton [11–14] to amide nitrogens. Protonation of the amide nitrogen has two profound effects: (1) it

weakens the amide bond; (2) the carbon atom of the protonated amide group becomes a likely target of a nucleophilic attack of nearby electron-rich groups.

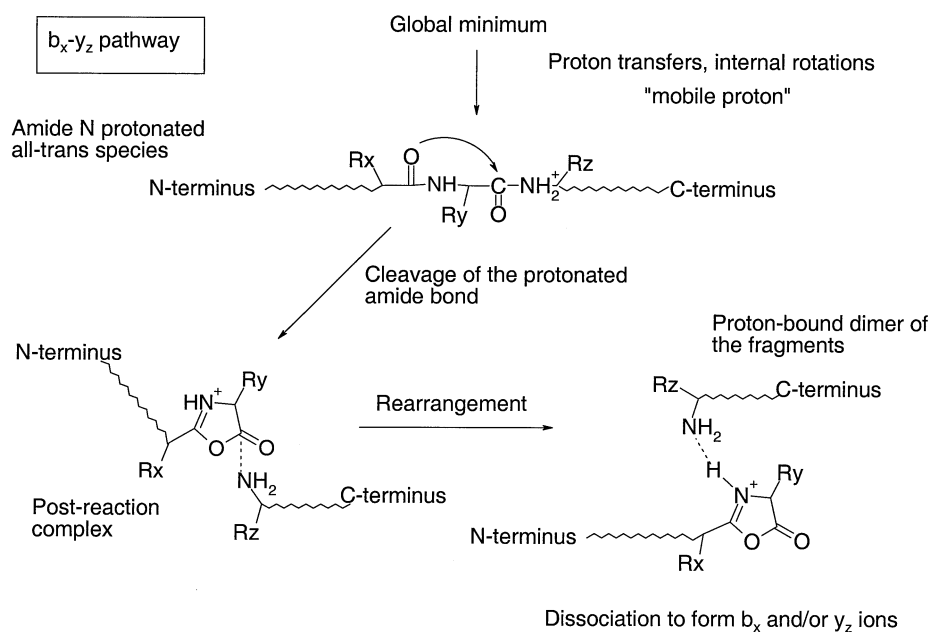
Amide nitrogen protonated species can dissociate by direct bond cleavage (Scheme 2), e.g., for the N-terminal amide bond of underivatized protonated peptides on the a_1-y_x pathway [15–17]. Under low-energy collision conditions, amide bonds except for the N-terminal one are usually cleaved in a more complex rearrangement (Scheme 2) involving nucleophilic attack of either the oxygen of the N-terminal neighbor amide bond (b_x-y_z pathway [17]) or the nitrogen of the N-terminal amino group (“diketopiperazine” pathway [18]) on the carbon of the protonated amide bond. (It is worth noting here that both pathways lead to formation of cyclic N-terminal products.) Determining the branching ratio of the b_x-y_z and “diketopiperazine” pathways for charge directed cleavage of the amide bonds is of significant importance for understanding the MS-MS spectra of protonated peptides.

The b_x-y_z Pathways

Nucleophilic attack by the oxygen of the N-terminal neighbor amide bond on the carbon center of the protonated amide bond on the b_x-y_z pathways [17] (compiled for a general oligopeptide in Scheme 3) leads to formation of a protonated oxazolone [19–23] derivative, while the detaching C-terminal fragment (amino acid or peptide) leaves the parent ion. Under low-energy collision conditions the loose complex of the protonated oxazolone derivative and the leaving C-terminal fragment has a finite lifetime, and can undergo a rearrangement which results in a proton-bound dimer of these species [17]. Under such circumstances the extra proton is shared by the two monomers, and dissociation of the proton-bound dimer will be determined by the thermochemistry [proton affinity (PA)] of the species involved leading to “integrated” formation of b_x and y_z ions [17]. The dissociation kinetics of the proton-bound dimer depends on the actual internal energy distribution, the proton affinity of its monomers, etc., and can be approximated by using a linear free-energy relationship [24, 25]

$$\ln(r(b_x/y_z)) \approx (PA_{N\text{-term}} - PA_{C\text{-term}})/RT_{\text{eff}} \quad (1)$$

where $r(b_x/y_z)$ is the ratio of the abundances of the b_x and y_z ions, $PA_{N\text{-term}}$ and $PA_{C\text{-term}}$ are the proton affinities (PA) of the neutral fragments of the corresponding b_x-y_z pathway (that is, PAs of an oxazolone derivative and a truncated peptide for the N- and C-terminal fragments, respectively), and T_{eff} denotes the “effective” temperature. Note that eq 1 is valid only if entropy effects of the two dissociation pathways (leading to b_x and y_z ions) are similar, there are no reverse activation barriers for the dissociations involved, and the dimer dissociates only by forming the



Scheme 3

oxazolone derivative and truncated peptide fragment (either of them is protonated). Since the entropy effects are not the same for the channels leading to b_x and y_z ions, eq 1 can be used only for semi-quantitative considerations on the $r(b_x/y_z)$ ion abundance ratios. Another limitation is that T_{eff} depends on the excitation method used in the MS-MS experiments. However, one does not need accurate T_{eff} values to approximate the $r(b_x/y_z)$ ion abundance ratio and an average value of 800 K leads to $r(b_x/y_z)$ values of 0.15, 0.3, 0.5, 1.9, 3.5, 6.6 if -3 , -2 , 1 , 1 , 2 , and 3 kcal/mol are assumed for $PA_{N\text{-term}}-PA_{C\text{-term}}$, respectively.

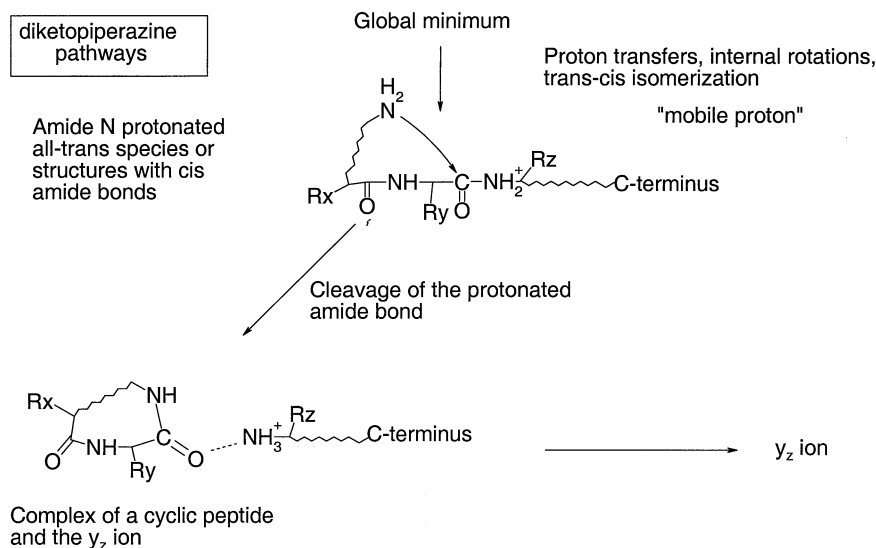
The general b_x-y_z pathways are feasible considering both energetic, kinetic, and entropy factors. The reactive configurations of the b_x-y_z pathways (*all-trans* amide nitrogen protonated species) are energetically accessible under low-energy collision conditions since the corresponding relative energies—calculated with respect to the most stable structure of the peptide protonated at the most favored protonation site—are in the range of 15–25 kcal/mol for peptides lacking arginine [14–16, 23, 26–28]. Theoretical studies [13, 14, 16, 26] on a few protonated peptides proved the existence and facility of proton transfer pathways that connect the most favored and the amide nitrogen protonation sites at internal energies well below the threshold energy of the lowest fragmentation pathways. Once the amide nitrogen protonated species are reached, concerted formation of the oxazolone ring and cleavage of the amide bond takes place via a 10–15 kcal/mol barrier [17, 23, 28] on a time-scale characteristic of a rearrangement-type reaction. In most of the amide nitrogen protonated species the oxygen of the N-terminal neighbor amide bond takes part in charge solvation of the $-\text{NH}_2^+$ -moiety bringing the nucleophilic oxygen close to the positive carbon

center. This ensures that entropy factors do not preclude amide bond dissociation on the b_x-y_z pathways.

The "Diketopiperazine" Pathways

Nucleophilic attack of the nitrogen of the N-terminal amino group on the carbon center of the protonated amide bond leads to the "diketopiperazine" pathways [18, 22], compiled for a general oligopeptide in Scheme 4). Formation of the cyclic peptide and cleavage of the amide bond take place in a concerted manner and yield primarily the complex of the protonated cyclic peptide and the C-terminal fragment (amino acid or truncated peptide). Since the proton affinities of cyclic peptides are much lower those of linear peptides, the extra proton transfers to the C-terminal fragment and the complex dissociates to form the y ion and the cyclic peptide as its neutral counterpart [22]. The size of the cyclic peptide depends on how far the cleaved amide bond locates from the N-terminus. For example, the neutral counterpart of y_{N-2} ions (N is the number of amino acid residues in the peptide) are diketopiperazine derivatives. For y_{N-3} , y_{N-4} , and y_{N-5} ions the corresponding neutrals are cyclo-tri-, cyclo-tetra-, and cyclopenta-peptides, respectively. In the following we refer to the various "diketopiperazine" pathways as diketopiperazine- y_{N-2} , diketopiperazine- y_{N-3} , etc.

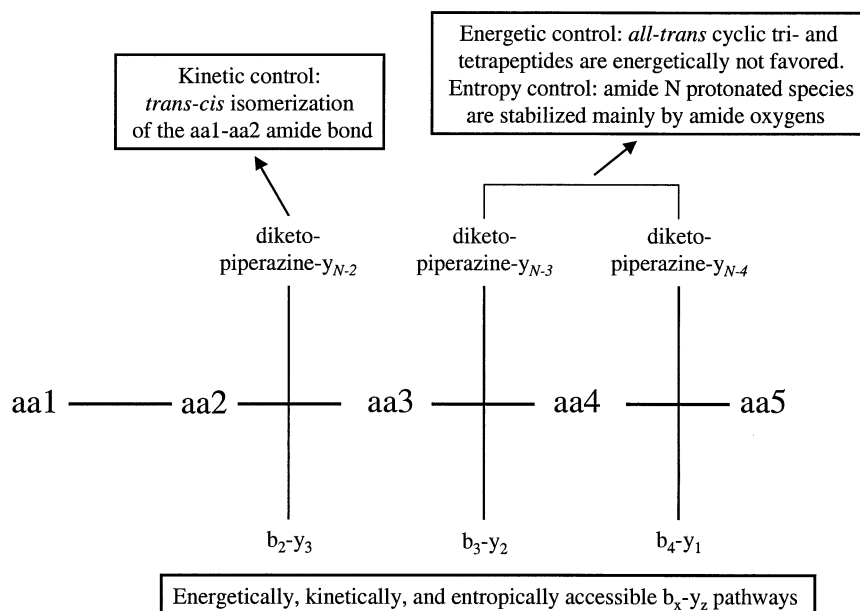
In the majority of the cases the general "diketopiperazine" pathways are controlled by either energetic or kinetic or entropy factors. To document this statement one has to distinguish between three major cases which involve the diketopiperazine- y_{N-2} , diketopiperazine- y_{N-M} (M is "average"), and diketopiperazine- y_{N-M} (M is "large") pathways. (The following



Scheme 4

considerations are schematically summarized in Scheme 5 for a pentapeptide). In the first case, the diketopiperazine derivatives—neutral counterparts of the y_{N-2} ions—contain two *cis* amide bonds. Since only one of these amide bonds is formed by the cyclization of the peptide, *cis-trans* isomerization of the N-terminal amide bond [16] has to take place on the diketopiperazine- y_{N-2} pathways prior to the nucleophilic attack in an energetically possible but *kinetically controlled* process [16]. In the case of the diketopiperazine- y_{N-M} (M is “average”) pathways *trans-cis* isomerization of the N-terminal amide bond is not necessary, the nitrogen of the terminal amino group can get close to the carbon center of the protonated amide bond to initiate forma-

tion of the cyclic peptide. However, small cyclic peptides accommodating only *trans* amide bonds suffer from significant ring strain leading to energetically disfavored fragmentation products. As the size of the cyclic peptide increases (cleavage far from the N-terminus), the cyclic peptides will suffer from less and less ring strain leading to energetically more favored diketopiperazine- y_{N-M} (M is “large”) pathways. However, these diketopiperazine- y_{N-M} pathways will be discriminated by entropy effects. This is due to the fact that the amide nitrogen protonated species are effectively solvated by nearby amide oxygens and the terminal amino group must compete with this kind of charge solvation in order to get close to the center of the protonated



Scheme 5

amide bond. While charge solvation of the $-\text{NH}_2^+$ -moiety by the terminal amino group is energetically feasible, the number of such species will be small compared to the large number of species where amide oxygens provide stabilization. This means that dissociation of protonated oligopeptides on the diketopiperazine- y_{N-M} pathways if the amide bond to be cleaved is located far from the N-terminus is disfavored because of entropy factors.

In the following we present detailed energetic and kinetic data on the major fragmentation pathways of protonated pentaalanine to validate the mechanistic considerations (Scheme 5) of the previous paragraphs. After describing the MS/MS spectrum of $\text{AAAAA}\cdot\text{H}^+$ we show that with modeling the various $b_x\text{-}y_z$ pathways one can fully explain the intensities of the major sequence ions leading to strong support to the mechanistic considerations involved. Some data will be presented also on the "diketopiperazine" pathways and dissociation channels leading to b ions with no oxazolone structure.

Understanding the Low-Energy Collision Induced Tandem Mass Spectra of Protonated Pentaalanine Based on Modeling the $b_x\text{-}y_z$ Pathways

The unimolecular and low energy collision induced fragmentation reactions of protonated AAAAA have

been investigated by Yalcin et al. [20]. The major peaks of the metastable ion mass spectrum correspond to the b_4 , b_5 , y_3 , b_3 , and y_2 ions with 53, 18, 14, 12, and 4 % of the total fragment ion abundance, respectively. The breakdown graph of protonated AAAAA [20] indicates that the intensity of the b_4 ion rapidly drops with increasing collision energy. In parallel, the b_3 and the y_3 ions become more abundant, reaching maximum intensity at 15 and 30 eV collision energies (laboratory scale). At even higher collision energies both b_3 and y_3 become less abundant in parallel with increasing b_2 and y_2 intensities. The abundance of the b_5 ion (non-sequence ion originated from loss of water) is small and nearly continuously drops as the collision energy is increased.

The appearance of a particular sequence ion in the MS/MS spectrum of protonated AAAAA depends on two major factors including the probability for the cleavage of the corresponding amide bond and mechanistic aspects that decide which fragment will keep the added proton during the spatial separation of the fragments. The dissociation probability depends on the energetic and kinetic accessibility of the reactive configurations and on the actual unimolecular rate constant of the bond cleavage. Under low-energy collision conditions the fate of the separating fragments is decided by the thermodynamics involved, that is, the fragment with larger proton affinity will usually keep the added proton. In the following we will analyze the

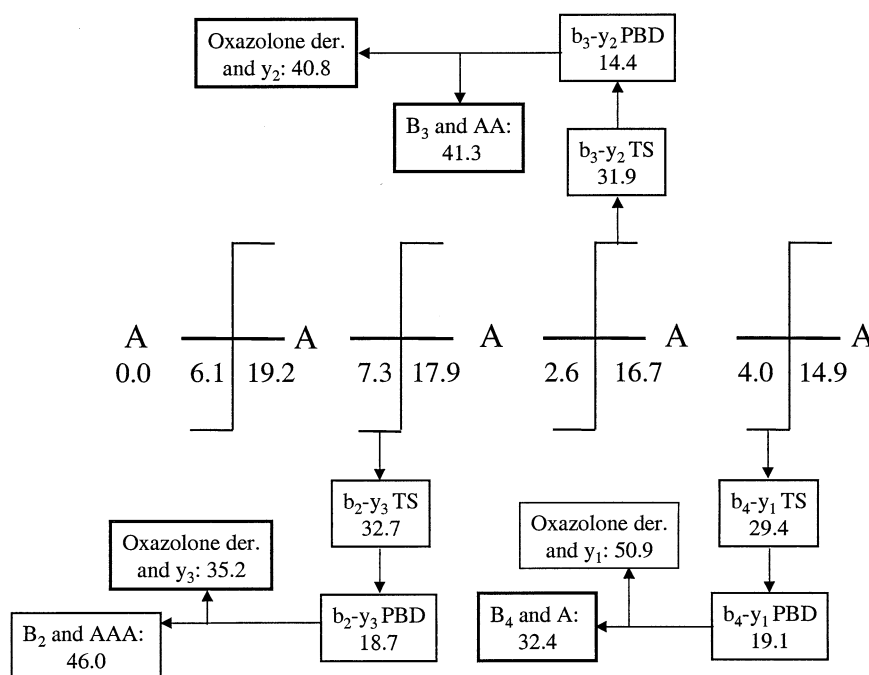


Figure 1. Energetics of the $b_x\text{-}y_z$ pathways of protonated pentaalanine. The relative energies (kcal/mol) of the *all-trans* pentaalanine species protonated at the N-terminal amino group, amide oxygens and nitrogens are noted at the N-terminus and at the corresponding amide bonds, respectively. For the amide bonds, first the oxygen and then the nitrogen energetics are shown. Relative energies are also presented for the transition structures ($b_x\text{-}y_z$ TS), proton-bound dimers ($b_x\text{-}y_z$ PBD) and final products of the $b_x\text{-}y_z$ pathways. The energetically preferred dissociation channel of the proton-bound dimers are highlighted by bold border.

Table 1. Computed total energies (Hartree, calculated at the B3LYP/6-31+G(d,p) level) of AAAAA species protonated at various protonation sites and of structures appearing on the b_x - y_z pathways. All species are fully optimized at the B3LYP/6-31+G(d,p) level of theory. For the b_x - b_z pathways total energies are presented for the corresponding transition structures (TS), proton-bound dimers (PBD), and the separated final products including b_x ions and oxazolone derivatives (N-terminal fragments) and A_x and A_xH^+ (C-terminal fragments)

Backbone protonation sites			
Protonation site	Total energy	Protonation site	Total energy
Terminal amino group	-1313.569053	Ala(1)-Ala(2)amide O	-1313.556803
Ala(2)-Ala(3)amide O	-1313.551668	Ala(3)-Ala(4)amide O	-1313.560316
Ala(4)-Ala(5)amide O	-1313.558743	Ala(1)-Ala(2)amide N	-1313.535382
Ala(2)-Ala(3)amide N	-1313.535425	Ala(3)-Ala(4)amide N	-1313.539047
Ala(4)-Ala(5)amide N	-1313.542179		
b_2 - y_3 pathway			
Species	Total energy	Species	Total energy
TS	-1313.511112	PBD	-1313.535018
AAA	-818.468262	AAA.H ⁺	-818.852503
Oxazolone der.	-494.649447	b_2	-495.016834
b_3 - y_2 pathway			
Species	Total energy	Species	Total energy
TS	-1313.512540	PDB	-1313.542016
AA	-571.120855	AA.H ⁺	-571.494210
Oxazolone der.	-741.999652	b_3	-742.372136
b_4 - y_1 pathway			
Species	Total energy	Species	Total energy
TS	-1313.517496	PBD	-1313.533036
A	-323.776274	A.H ⁺	-324.132674
Oxazolone der.	-989.350542	b_4	-989.732896

b_x - y_z fragmentation pathways of protonated pentalanine considering the most important points of this general scheme for the different dissociation channels including b_2 - y_3 , b_3 - y_2 , and b_4 - y_1 . (The a_1 - y_4 pathway is not active, so no details are presented for this dissociation channel.)

The results of the theoretical modeling of the b_x - y_z pathways of protonated AAAAA are summarized in Figure 1 and Table 1. Scan of the potential energy surface (PES) of protonated AAAAA leads to useful information on the relative stability of the various protonation sites including the N-terminal amino group, amide oxygens and nitrogens. Density functional calculations (Figure 1) indicate that the global minimum is one of the many N-terminal amino protonated species. Amide oxygen protonated species including the A(1)-A(2), A(2)-A(3), A(3)-A(4), and A(4)-A(5) amide oxygen protonation sites, lie at 6.1, 7.3, 2.6, and 4.0 kcal/mol relative energies, respectively. It is worth noting here that the A(3)-A(4) and A(4)-A(5) amide oxygen protonated species have quite low relative energies (2.6 and 4.0 kcal/mol, respectively). This is in contradiction with the general view [29] that as the size of the peptide increases the terminal amino protonated species will be over-stabilized compared with the amide oxygen protonated species because of the very efficient charge solvation of the $-NH_3^+$ group. This effect is under further study in our laboratory since amide oxygen protonated species play

major role in the gas phase H/D exchange reactions of protonated peptides [30, 31].

The various b_x - y_z pathways are initiated from amide nitrogen protonated species which have significantly higher relative energies than that of the most stable N-terminal amino and amide oxygen protonated structures (Figure 1). Protonation at the A(1)-A(2), A(2)-A(3), A(3)-A(4), and A(4)-A(5) amide nitrogen protonation sites requires at least 19.2, 17.9, 16.7, and 14.9 kcal/mol internal energies, respectively. These data indicate that protonation at the amide nitrogen becomes energetically more feasible for peptide bonds that are located close to the C-terminus. This means that if the kinetics of the various proton transfer pathways connecting the most stable and the amide nitrogen protonated species do not discriminate amongst the amide nitrogens, the dissociation probability of the amide bonds will increase if the amide bond is located closer to the C-terminus.

Other factors that determine the dissociation probability are the energetics of the b_x - y_z transition structures and the magnitude of the internal energy dependent unimolecular rate constants. The data of Figure 1 suggest that the relative energies of the b_x - y_z transition structures lie in the narrow 29–33 kcal/mol range and decrease for amide bonds lying closer to the C-terminus similarly to the tendency found for the energetics of the amide nitrogen protonated species. The actual relative

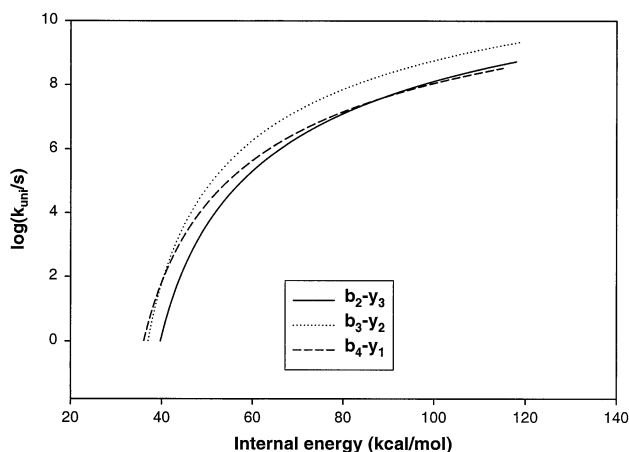


Figure 2. Unimolecular rate constants calculated for the b_x - y_z pathways.

energies for the b_2 - y_3 , b_3 - y_2 , and b_4 - y_1 TSs are 32.7, 31.9, and 29.4 kcal/mol, respectively. This tendency again suggests that the dissociation probability increases as the particular amide bond locates closer to the C-terminus.

RRKM calculations (Figure 2) indicate only small differences between the magnitudes of the unimolecular rate constants calculated for the b_x - y_z pathways. In the 40–80 kcal/mol internal energy interval the b_2 - y_3 pathway seems to be slower than b_3 - y_2 and b_4 - y_1 while above 80 kcal/mol internal energy the b_3 - y_2 pathway is more facile than the other two.

Together with the energetic considerations, the RRKM results suggest that one expects discrimination between the b_x - y_z pathways of protonated AAAAA only at very low internal energies just above the dissociation threshold where the b_4 - y_1 pathway is favored compared with the b_2 - y_3 or b_3 - y_2 .

The theoretical results on the branching ratio of the b_x - y_z pathways for protonated AAAAA are in nice agreement with the MI and low-energy collision condition data. The MI spectrum of protonated AAAAA indicates that the dissociation probability increases for amide bonds in the A(2)–A(3), A(3)–A(4), and A(4)–A(5) series since the actual percentages for the b_2 / y_3 , b_3 / y_2 , and b_4 / y_1 ion pairs are 14, 16, and 53, respectively. The activities of the b_2 - y_3 and b_3 - y_2 pathways are close to one another due to the similar energetics and kinetics of the dissociation (see above). At low internal energies (manifested under metastable ion conditions) the b_4 - y_1 pathway is favored by both energetics and kinetics resulting in dominance of the b_4 ion.

The above considerations on the branching ratio of the b_x - y_z pathways are also in line with the breakdown graph [20] of protonated AAAAA. For example, at 5 eV collision energy (laboratory scale) the actual percentages for the b_2 / y_3 , b_3 / y_2 , and b_4 / y_1 ion pairs are 4, 16, and 69, respectively, which means that the MS-MS spectrum is dominated by the b_4 ion (y_1 is missing, for the reason given later). Similar trends rule up to 20 eV collision energy while from 25 eV collision energy the

b_2 / y_3 and b_3 / y_2 ion pairs become more abundant than b_4 / y_1 . This latter fact can be explained by considering the $b_n \rightarrow b_{n-1}$ and $y_n \rightarrow y_{n-1}$ reactions which will be more facile as the internal energy of ions increases, depleting b_4 , b_3 , and y_3 .

While the branching ratio of the various b_x - y_z pathways is understood for the low energy MS-MS spectrum of protonated AAAAA, one still has to explain the abundance ratio of the b_x and y_z ions for each of the b_2 - y_3 , b_3 - y_2 , and b_4 - y_1 channels. To this end we will apply eq 1 and approximate the $r(b_2/y_3)$, $r(b_3/y_2)$, and $r(b_4/y_1)$ ion abundance ratios using free energy relationships.

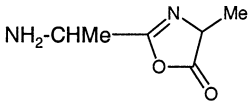
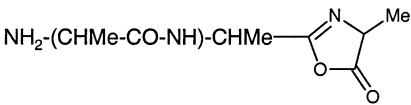
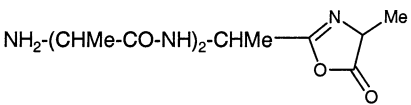
To use eq 1 one needs reasonable proton affinity values of the corresponding oxazolone derivatives and truncated peptides. While experimental data are available on the PA of A [32] and AA [33] (214.2 and 226.3 kcal/mol, respectively), there are no reported PA values for oxazolones. Therefore, we have calculated the PA of each corresponding molecule at the reasonable B3LYP/6-31+G(d,p) theoretical level. The density functional calculations on the PA of A and AA give good agreement with the corresponding experimental data [32, 33] indicating a sufficient level of theory is utilized. The computed data (Table 2) show that the PA of the oxazolone derivatives increases significantly for the series derived from the b_2 , b_3 , and b_4 ions. Also, the PA of the C-terminal fragment A_X ($X = 1,3$) species increases as X gets larger.

Comparing the PAs of the oxazolone (NH_2 -CHMe-COCONCHMe) derived from the b_2 ion and that of AAA (222.3 and 233.1 kcal/mol, respectively, Table 2) indicates that under low-energy collision conditions only y_3 ions are formed on the b_2 - y_3 pathway. This is due to the fact that the difference between the PAs of the corresponding neutrals is more than 10 kcal/mol and eq 1 leads to a very small b_2/y_3 ion abundance ratio.

Comparing the PAs of the oxazolone (NH_2 -CHMe-CO-NH)-CHMe-COCONCHMe derived from the b_3 ion and that of AA (226.0 and 225.4 kcal/mol, respectively, Table 2) indicates that under low-energy collision conditions formation of the b_3 ions is slightly favored compared with that of y_2 in reasonable agreement with the MI spectrum which show the presence of both b_3 and y_2 ions (12 and 4% of the total fragment ion abundance, respectively). The PA of the oxazolone (NH_2 -(CHMe-CO-NH) $_2$ -CHMe-COCONCHMe) derived from the b_4 ion is much larger than that of A. This means that formation of the b_4 ion is favored on the b_4 - y_1 pathway in agreement with the experimental data which show an abundant b_4 ion and no y_1 .

It seems to be reasonable to comment on the energy levels of the final products of the b_x - y_z pathways. The energetically preferred fragmentation products are at 32–35 kcal/mol relative energy (Figure 1) for the b_2 - y_3 and b_4 - y_1 pathways while the b_3 - y_2 exits lie at 41–42 kcal/mol. For the b_2 - y_3 and b_4 - y_1 cases the PA of one of the fragments (Table 2) is much

Table 2. Calculated proton affinities (kcal/mol) of oxazolone derivatives, alanine and small peptides of alanine. All calculations were performed at the B3LYP/6-31+G(d,p) level of theory. The identity of the protonated form of the neutrals is denoted (under heading 'MS/MS ion') according to the nomenclature used for the MS-MS spectra of peptides.

Pathway	C-terminal fragment			N-terminal fragment		
	Neutral	MS/MS ion	PA	Neutral	MS/MS ion	PA
b ₂ -y ₃		b ₂	222.3	AAA	y ₃	233.1
b ₃ -y ₂		b ₃	226.0	AA	y ₂	225.4
b ₄ -y ₁		b ₄	232.6	A	y ₁	214.6

larger than that of the other (offering an energetically preferred way of dissociation of the proton-bound dimer) while for the b₃-y₂ pathway the PAs of both the oxazolone derivative and AA are smaller than that of AAA or NH₂-(CHMe-CO-NH)₂-CHMe-COCONCHMe (oxazolone derived from b₄). However, the fact that the b₃-y₂ final products are energetically less favored than those formed on the b₂-y₃ and b₄-y₁ pathways, does not preclude formation of the corresponding b₃ and y₂ ions indicating that the fragmenting species have significant internal energies.

The "Diketopiperazine" Pathways of Protonated AAAAA

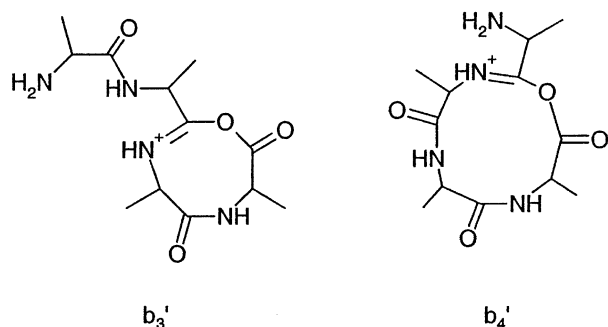
While the MI and low-energy collision induced mass spectra of protonated pentaalanine can be understood based on considerations on the b_x-y_z pathways and according to the general discussion of the branching ratio of the b_x-y_z and "diketopiperazine" channels the later is disfavored in most of the cases, it seems to be interesting to evaluate some details of the diketopiperazine-y₂ and diketopiperazine-y₁ pathways for protonated pentaalanine. The kinetic control [16] of the diketopiperazine-y₃ pathway is not described here in detail; we just note that the attacking N-terminal amino group can get close to the carbon center of the protonated A(2)-A(3) amide bond if the A(1)-A(2) amide bond is in the *cis* isomerization state. The necessary *trans-cis* isomerization involves amide nitrogen protonated species under kinetic control in most of the cases. There is no such restriction on the diketopiperazine-y₂ and di-

ketopiperazine-y₁ pathways since the attacking N-terminal amino nitrogen can get close to the protonated A(3)-A(4) and A(4)-A(5) amide bonds without *trans-cis* isomerization of amide bonds. However, the corresponding cyclic tri- and tetra-peptides formed as neutral counterparts of the y₂ and y₃ ions, respectively, are energetically not favored due to the large ring strain caused by accommodation of all the amide bonds in the *trans* isomerization state. This means, that even the favored final products (neutral cyclic peptides and the y₂ or y₁ ion) on the diketopiperazine-y₂ and diketopiperazine-y₁ pathways have high relative energies at 48.8 and 44.8 kcal/mol, respectively. For the diketopiperazine-y₁ pathway we have located both the reactive configuration and the transition structure which lie at 22.4 and 47.1 kcal/mol relative energies and are much less favored than the corresponding b₄-y₁ species (14.9 and 24.9 kcal/mol relative energy, respectively).

Do All b Ions of Protonated AAAAA have the Oxazolone Structure?

Protonated amide nitrogens can be charge-solvated by various electron-rich groups involving mostly the N-terminal neighbor and other amide oxygens. In some circumstances not only the N-terminal neighbor amide oxygen can get close to the carbon center of the protonated amide bond but also other amide oxygens can be involved in formation of the b₃ and b₄ ions. Of course, such reactions lead to ions which do not have the

classical oxazolone structure but contain larger rings like



(The notation b_x' is used to represent species having different structural motifs than the classical oxazolone ring.) Our calculations indicate that b_3' and b_4' are less favored than b_3 and b_4 by 26.6 and 19.9 kcal/mol energy, respectively. This indicates that the b_x ions of protonated pentaalanine have the classical oxazolone structure and the pathways leading to b_3' and b_4' ions can not compete with the general b_x - y_z channels.

Conclusions

The mechanism of amide bond cleavage in protonated oligopeptides was discussed in the present paper paying special attention to the energetic, kinetic, and entropy factors determining the branching ratio of the b_x - y_z and diketopiperazine pathways. The most important result are summarized as follows:

1. Energetic, kinetic, and entropy considerations indicate that the b_x - y_z pathways [17] are favored against the diketopiperazine [18] channels in the majority of the cases.
2. The general b_x - y_z pathways are energetically, kinetically, and entropically accessible under low-energy collision conditions.
3. Formation of the y_{N-2} (N = number of amino acid residues) ion on the diketopiperazine pathway is kinetically disfavored because of the *trans-cis* isomerization [16] necessary to form the corresponding reactive configuration.
4. Formation of the y_{N-M} (M is "average") ions on the diketopiperazine pathways is energetically disfavored because the corresponding neutrals—cyclic peptides accommodating a few *trans* amide bonds—suffer from significant ring strain.
5. Formation of the y_{N-M} (M is "large") ions on the diketopiperazine pathways is entropically disfavored because the corresponding protonated amide N s are solvated by the many nearby amide oxygens keeping the N-terminal amino group far from the

positive carbon to be attacked to initiate cleavage of the amide bond.

6. Modeling the b_x - y_z pathways provides a *semi-quantitative* explanation for the metastable ion and low-energy collision induced mass spectra of protonated AAAAA.
7. Both the amide nitrogen protonated structures (reactive configurations for the amide bond cleavage) and the corresponding b_x - y_z transition structures are energetically more favored if protonation occurs closer to the C-terminus, e.g., considering these points the Ala(4)–Ala(5) amide bond is more favored than Ala(3)–Ala(4), and Ala(3)–Ala(4) is more favored than Ala(2)–Ala(3). RRKM calculations indicate only small differences between the rate constants for the b_x - y_z pathways. These facts explain the increasing abundances observed for the b_2/y_3 , b_3/y_2 , and b_4/y_1 ion pairs in the metastable ion and low-energy collision induced mass spectra.
8. A linear free-energy relationship (eq 1) is used to approximate the ratio of the b_x and y_z ion on the particular b_x - y_z pathways. Applying the necessary proton affinities such considerations satisfactorily explain the dominance of the b_4 ion over y_1 and why the b_3 ion is more abundant than y_2 (both b_3 and y_2 are present in the mass spectra).
9. The energetics of the "diketopiperazine" pathways indicate that the b_3 - y_2 and b_4 - y_1 channels are favored against diketopiperazine- y_2 and diketopiperazine- y_1 .
10. Large ring containing alternative structures proposed for the b_3 and b_4 ions are energetically less favored than the classical oxazolone species.

The validity of the mechanistic speculations of the present paper are under further study in our laboratory on peptides like GGGG, Ac-AAA, AAAA, Leu-enkephaline, etc.

Acknowledgments

BP is grateful to Professor A. G. Harrison for providing detailed data on the breakdown graph of protonated AAAAA.

References

1. Fenn, J. B.; Mann, M.; Meng, C. K.; Wong, S. F.; Whitehouse, C. M. Electrospray Ionization for Mass-Spectrometry of Large Biomolecules. *Science* **1989**, *246*, 64.
2. Karas, M.; Hillenkamp, F. Laser Desorption Ionization of Proteins with Molecular Masses Exceeding 10,000 Da. *Anal. Chem.* **1988**, *60*, 2299.
3. Roepstorff, P.; Fohlman, J. Proposal for a Common Nomenclature for Sequence Ions in Mass Spectra of Peptides. *Biomed. Mass Spectrom.* **1984**, *11*, 601.

4. Biemann, K. Contributions of Mass Spectrometry to Peptide and Protein Structure. *Biomed. Env. Mass Spectrom.* **1988**, *16*, 99.
5. Mann, M.; Wilm, M. Error-Tolerant Identification of Peptides in Sequence Databases by Peptide Sequence Tags. *Anal. Chem.* **1994**, *66*, 4390.
6. Eng, J. K.; McCormack, A. L.; Yates, J. R. III. An Approach to Correlate Tandem Mass Spectra Data of Peptides with Amino Acid Sequences in a Protein Database. *J. Am. Soc. Mass Spectrom.* **1994**, *5*, 976.
7. Perkins, D. N.; Pappin, D. J. C.; Creasy, D. M.; Cottrell, J. S. Probability-Based Protein Identification by Searching Sequence Databases Using Mass Spectrometry Data. *Electrophoresis* **1999**, *20*, 3551–3567.
8. Clauser, K. R.; Baker, P. R.; Burlingame, A. L. Role of Accurate Mass Measurement (± 10 ppm) in Protein Identification Strategies Employing MS or MS/MS and Database Searching. *Anal. Chem.* **1999**, *71*, 2871.
9. Baer, T.; Hase, W. L. *Unimolecular Reaction Dynamics*; Oxford University Press: Oxford, 1996.
10. Frisch, M. J. Gaussian-98, Rev. A9. Gaussian, Inc.: Pittsburgh PA, 1995.
11. Dongré, A. R.; Jones, J. L.; Somogyi, Á.; Wysocki, V. H. Influence of Peptide Composition, Gas-Phase Basicity, and Chemical Modification on Fragmentation Efficiency: Evidence for the Mobile Proton Model. *J. Am. Chem. Soc.* **1996**, *118*, 8365.
12. Harrison, A. G.; Yalcin, T. Proton Mobility in Protonated Amino Acids and Peptides. *Int. J. Mass Spectrom. Ion Processes* **1997**, *165/166*, 339.
13. Csonka, I. P.; Paizs, B.; Lendvay, G.; Suhai, S. Proton Mobility in Protonated Peptides: A Joint Molecular Orbital and RRKM Study. *Rapid Commun. Mass Spectrom.* **2000**, *14*, 417.
14. Paizs, B.; Csonka, I. P.; Lendvay, G.; Suhai, S. Proton Mobility in Protonated Glycylglycine and N-Formylglycylglycinamide: A Combined Quantum Chemical and RRKM Study. *Rapid Commun. Mass Spectrom.* **2001**, *15*, 637.
15. Paizs, B.; Suhai, S. Theoretical Study of the Main Fragmentation Pathways for Protonated Glycylglycine. *Rapid Commun. Mass Spectrom.* **2001**, *15*, 651.
16. Paizs, B.; Suhai, S. Combined Quantum Chemical and RRKM Modeling of the Main Fragmentation Pathways of Protonated GGG. I. Cis-trans Isomerization Around Protonated Amide Bonds. *Rapid Commun. Mass Spectrom.* **2001**, *15*, 2307.
17. Paizs, B.; Suhai, S. Combined Quantum Chemical and RRKM Modeling of the Main Fragmentation Pathways of Protonated GGG. II. Formation of b_2 , y_1 , and y_2 Ions. *Rapid Commun. Mass Spectrom.* **2002**, *16*, 375.
18. Cordero, M. M.; Houser, J. J.; Wesdemiotis, C. The Neutral Products Formed During Backbone Fragmentations of Protonated Peptides in Tandem Mass Spectrometry. *Anal. Chem.* **1993**, *65*, 1594.
19. Yalcin, T.; Khouw, C.; Csizmadia, I. G.; Peterson, M. R.; Harrison, A. G. Why are b Ions Stable Species in Peptide Spectra? *J. Am. Soc. Mass Spectrom.* **1995**, *6*, 1165.
20. Yalcin, T.; Csizmadia, I. G.; Peterson, M. B.; Harrison, A. G. The Structure and Fragmentation of B_n ($n \geq 3$) Ions in Peptide Spectra. *J. Am. Soc. Mass Spectrom.* **1996**, *7*, 233.
21. Nold, M. J.; Wesdemiotis, C.; Yalcin, T.; Harrison, A. G. Amide Bond Dissociation in Protonated Peptides. Structures of the N-terminal Ionic and Neutral Fragments. *Int. J. Mass Spectrom. Ion Processes* **1997**, *164*, 137.
22. Polce, M. J.; Ren, D.; Wesdemiotis, C. Dissociation of the Peptide Bond in Protonated Peptides. *J. Mass Spectrom.* **2000**, *35*, 1391.
23. Paizs, B.; Lendvay, G.; Vékey, K.; Suhai, S. Formation of b_2^+ Ions from Protonated Peptides: An ab Initio Study. *Rapid Commun. Mass Spectrom.* **1999**, *13*, 525.
24. Paizs, B.; Suhai, S. Towards Understanding Some Ion Intensity Relationships for the Tandem Mass Spectra of Protonated Peptides. *Rapid Commun. Mass Spectrom.* **2002**, *16*, 1699.
25. Harrison, A. G. Linear Free Energy Correlations in Mass Spectrometry. *J. Mass Spectrom.* **1999**, *34*, 577.
26. Csonka, I. P.; Paizs, B.; Lendvay, G.; Suhai, S. Proton Mobility and Main Fragmentation Pathways of Protonated Lysylglycine. *Rapid Commun. Mass Spectrom.* **2001**, *15*, 1457.
27. Jegorov, A.; Paizs, B.; Zabka, M.; Kuzma, M.; Giannakopoulos, A. E.; Derrick, P. J.; Havlicek, V. Profiling of Cyclic Hexadepsipeptides Roseotoxins Synthesized in Vitro and in Vivo: A Combined Tandem Mass Spectrometry and Quantum Chemical Study. *Eur. J. Mass Spectrom.* **2003**, *9*, 105.
28. Paizs, B.; Suhai, S.; Harrison, A. G. Experimental and Theoretical Investigation of the Main Fragmentation Pathways of Protonated H-Gly-Gly-Sar-OH and H-Gly-Sar-Sar-OH, in press.
29. Campbell, S.; Rodgers, M. T.; Marzluff, E. M.; Beauchamp, J. L. Deuterium Exchange Reactions as a Probe of Biomolecule Structure. Fundamental Studies of Gas Phase H/D Exchange Reactions of Protonated Glycine Oligomers with D_2O , CD_3OD , CD_3CO_2D , and ND_3 . *J. Am. Chem. Soc.* **1995**, *117*, 12840.
30. Paizs, B.; Lendvay, G.; Suhai, S. Towards Understanding the Mechanism of Gas Phase Hydrogen/Deuterium (H/D) Exchange Reactions of Protonated Peptides I. Reactions of Protonated Glycylglycine with D_2O , unpublished.
31. Wyttenbach, T.; Paizs, B.; Barran, P.; Brechi, L.; Liu, D.; Suhai, S.; Wysocki, V. H.; Bowers, M. T. The Effect of the Initial Water of Hydration on the Energetics, Structures and H/D-Exchange Mechanism of a Family of Pentapeptides: An Experimental and Theoretical Study, in press.
32. Harrison, A. G. The Gas-Phase Basicities and Proton Affinities of Amino Acids and Peptides. *Mass Spectrom. Rev.* **1997**, *116*, 201.
33. Cassady, C. J.; Carr, S. R.; Zhang, K.; Chung-Phillips, A. Experimental and ab Initio Studies on Protonations of Alanine and Small Peptides of Alanine and Glycine. *J. Org. Chem.* **1995**, *60*, 1704.